Materials Research Proceedings 41 (2024) 2182-2189 https://doi.org/10.21741/9781644903131-240

Influence of manufacturing defaults on the behavior of 3D printed lattice structures with a multiscale data-driven approach

COURT Clément[1,a*], MARENIC Eduard[1,b] and PASSIEUX Jean-Charles[1,c]

[1]Institut Clément Ader (ICA), Université de Toulouse, INSA-ISAE-Mines Albi-UPS-CNRS, Toulouse, France

[a]ccourt@insa-toulouse.fr, [b]marenic@insa-toulouse.fr, [c]passieux@insa-toulouse.fr

Keywords: Lattice, Additive Manufacturing, Data-Driven, Multiscale, Digital Twins

Abstract. The inherent multiscale (MS) complexity of lattice materials necessitates specialized modeling techniques to predict their mechanical behavior accurately and efficiently. A combination of the multiscale finite element method (*e.g.* FE²), with a Data-Driven paradigm, leads to Multi Scale Data-Driven (MSDD) modeling procedure to simulate the behavior of these materials. On top of the inherent complexity of these materials, limitations of the Laser Powder Bed Fusion (LPBF) manufacturing process result in geometrical imperfections of the manufactured materials giving rise to so called *as-manufactured* configuration. Furthermore, theses imperfections have significant influence on the mechanical behavior and introduce biases and variance from expected behavior based on the modeling with initially designed lattice material, so called *as-designed* configuration. The proposed research is the first step in the reduction of the cost of MSDD approach by aligning the model's accuracy with the manufacturing capabilities. The aim is to exploit the inherent variance in *as-manufactured* lattice material and to minimizing the material database to the essential material state points. To that end, in this work, using X-ray tomography, we create digital twins of various *as-manufactured* aluminum lattice unit cells and perform a number of simulations. The goal is to get further understanding of the variance in mechanical behavior resulting from geometrical variations and defects. These results will be further used to enhance the efficiency of the MSDD approach with no compromise on predictive capabilities.

Introduction

Lattice materials. The rapid development of additive manufacturing in particular Laser Powder Bed Fusion (LPBF), enabled the design at the material scale in order to create, so called, lattice materials. These materials are a subset of cellular materials [1] and exhibit a high stiffness-over-mass ratio, making them particularly attractive for aerospace applications [2]. Lattice samples shown in this work were manufactured with Selective Laser Melting (SLM) [3] process on the machine SLM®125.

Manufacturing process depends on several parameters, namely laser displacement velocity, laser power, laser spot size, the powder constitutive material or its grain size. There is obviously a number of influential factors, some of them are random and their interaction and effects are still not completely understood. This further leads to differences between the *as-designed* and *as-manufactured* configurations in terms of relative volume and shape.

In [4], the authors enlighten different types of defects (Fig. 1): local cross-section variations of struts, waviness, porosity and even notches. In their work, the authors study the influence of these

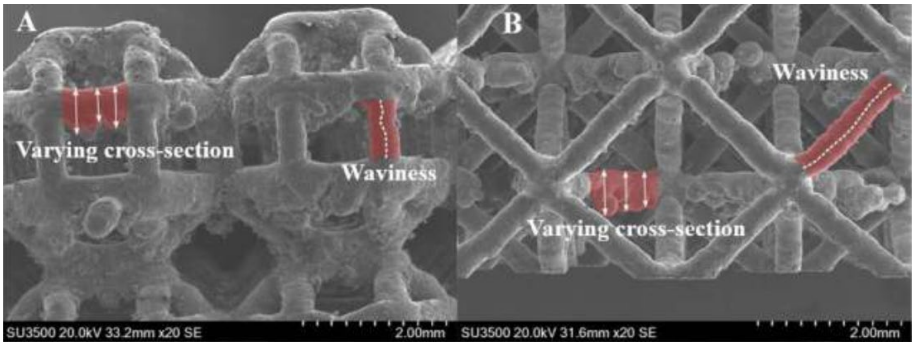

Fig. 1: Scanning Electron Microscope images of rhombicuboctahedron (A) and regular octet (B) lattices enlightening manufacturing defects [4].

defects on the mechanical behavior of lattice material samples. They classify the defects and introduce a statistical distribution in a beam-based finite element model.

On the contrary, in this work we avoid the defects classification and we focus on creating the three-dimensional (3D) finite element (FE) models. These models are built from the 3D images obtained from the X-ray tomography of the real manufactured lattice samples.

Multiscale methods for lattice materials. Lattice materials represent complex cellular structures composed of repeating unit cells. If we add on top of this rather complex structure the details of the *as-manufactured* configuration (geometry variations described above), prohibitive computational costs render the direct numerical simulation virtually impossible. This type of problems where two distinguished length scales exist – local unit cells at the mesoscopic scale and global structure at the macroscopic scale – are often modeled using MS approach, *e.g.* FE² [5]. This method solves the macroscopic boundary value problem of the global structure and the local problem of the unit cell considered as a Representative Volume Element (RVE), as illustrated in Fig. 2.

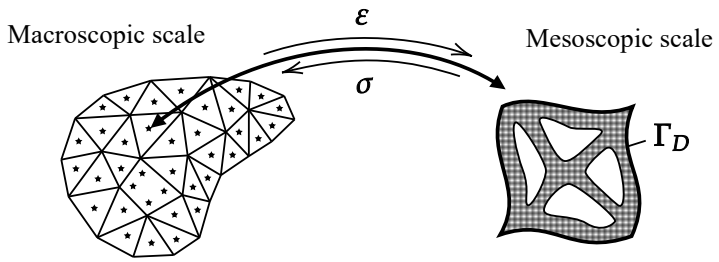

Fig. 2: Multiscale mechanical problem illustration

Contrary to classical FE methods, the macroscopic problem is not driven by a material constitutive law, but by the homogenized results of mesoscopic scales problems of the RVE. Typically, the effective material behavior at the macroscopic scale is obtained by homogenizing the stress field of the RVE loaded with a given strain state, for each integration point on the macroscale. Although this kind of procedure can be parallelized due to independent mesoscopic problems, one needs to run a generally non-linear simulation for each integration points and each load increment of the macroscopic problems. Moreover, linear perturbation evaluations on the RVE are needed to obtain the tangent operator for the macroscopic problem. To reduce the number of simulations on RVE it is possible to reuse the previously calculated solutions using model reduction techniques or machine learning [6]. In the following work we will use an alternative approach based on Data-Driven simulations.

Data-Driven Computational Mechanics. In 2015, Kirchdoerfer and Ortiz [7] introduced a formulation of the boundary value problem where the material constitutive law model is replaced by data. In this context one still needs to verify the kinematic compatibility condition (Eq. 1) and the static equilibrium condition (Eq. 2).

$$\boldsymbol{\varepsilon} = 1/2\ (\nabla \mathbf{q} + (\nabla \mathbf{q})^{\mathrm{T}}) \tag{1}$$

$$\mathrm{div}(\boldsymbol{\sigma}) + \mathbf{f}_{\mathrm{v}} = \mathbf{0} \tag{2}$$

where $\mathbf{q}$, $\boldsymbol{\varepsilon}$, $\boldsymbol{\sigma}$, $\mathbf{f}_{\mathrm{v}}$ are displacements field, strain field, stress field and external forces, respectively. However, the material behavior is now encoded as a cloud of points given as couples of strain and stress tensors ($\boldsymbol{\varepsilon}$, $\boldsymbol{\sigma}$). The space where the data points are defined is called the *phase space* and is usually noted *Z*, it has 12 dimensions (6 for the strain components and 6 for the stress components, both in Voigt notation). Solution to the boundary value problem is obtained by minimizing a distance *d* in Z, between the admissible mechanical states from the set called *C* – which verify Eq. 1 and Eq. 2 – and the states from the material database called *D*. To that end, we use an energy norm, that is, the squared distance between two points of the phase space $(\boldsymbol{\varepsilon}_{\mathrm{c}}, \boldsymbol{\sigma}_{\mathrm{c}}) \in C$ and $(\boldsymbol{\varepsilon}_{\mathrm{d}}, \boldsymbol{\sigma}_{\mathrm{d}}) \in D$ is given by

$$d^2 = 1/2\ ((\boldsymbol{\varepsilon}_{\mathrm{c}} - \boldsymbol{\varepsilon}_{\mathrm{d}}) : \mathbb{C} : (\boldsymbol{\varepsilon}_{\mathrm{c}} - \boldsymbol{\varepsilon}_{\mathrm{d}})) + 1/2\ ((\boldsymbol{\sigma}_{\mathrm{c}} - \boldsymbol{\sigma}_{\mathrm{d}}) : \mathbb{C}^{-1} : (\boldsymbol{\sigma}_{\mathrm{c}} - \boldsymbol{\sigma}_{\mathrm{d}})) \tag{3}$$

where $\mathbb{C}$ is a purely numerical Hooke-like operator.

In this work we turn to the combination of FE² MS strategy with the Data-Driven paradigm [8], leading to MSDD method. The goal is to substitute the systematic online simulations on the RVE by the nearest neighbor search in terms of the distance defined in Eq. 3 and within the previously created material database. This makes the MSDD approach a good candidate to reduce the costs of the FE² method. We note that the material database is in the MSDD context usually created before in the offline phase, however it is still possible to add new data points in the material database by simulation of the RVE if necessary [9]. The principle obstacle within MSDD solver is the nearest neighbor search step which can be expensive if the database is large. Some of the standard efficient searching methods are readily available to accelerate this step, such as tree searching (*kd*-trees, *k*-means trees, etc.), see also some other techniques proposed in [10].

In our work we would like to explore the possibility of taking into account the variance inherent to the manufacturing process in order to reduce the size of the material database and avoid expensive and over-sampled material databases. More precisely, the overall goal is to propose a method to use the knowledge of the manufacturing uncertainties to filter an over-sampled database while keeping the same predictive capabilities at the macroscopic scale. In this work the first step considers exploiting X-ray tomography images and creation of digital twins of various *as-manufactured* aluminum lattice unit cells. With the accurate 3D description in hands, we tend to perform a number of RVE simulations with *as-manufactured* configuration to get further understanding of the variance in mechanical behavior resulting from geometrical variations and defects. These results will be used in our further work to enhance the efficiency of the MSDD approach.

Methods

Manufacturing and 3D imagery. For this work, lattice sample (Fig. 3b) was manufactured with Selective Laser Melting (SLM) process on the machine SLM®125 and using an aluminum alloy powder AlSi7Mg0,6 according to the norm DIN EN 1706 / EN AC-42200. A unit cell in this sample is CFCC type, hybrid cell composed of the Face Centered Cubic and Center cross-like reinforcement (Fig. 3a). The *as-designed* unit cells have a side length of 4.069 mm and a relative volume of 16.81% (Fig. 3a). The use of X-ray tomography and 3D imagery with 18µm voxel size enabled to reconstruct the surfaces of the *as-manufactured* unit cells (Fig. 3c).

(a): *As-designed* CFCC unit cell.

(b): Lattice sample manufactured by SLM.

(c): Reconstructed surfaces of a unit cell of the manufactured sample.

Fig. 3: Sample and unit cells illustrations.

Creation of RVEs from digital twins. Digital twins are numerical models based on real structures. Firstly, the unit cells are extracted from the whole sample 3D image and treated separately. As can be seen from Fig. 3c reconstructed surfaces of the manufactured unit cell with 18µm voxel size are rough and too rich for intended FE modeling. To be able to create a 3D finite element mesh, it was necessary to apply a filter on the images to artificially smoothen the surfaces. This filtering must be as low as possible to minimize the modification of the extracted cell's geometry. After the images are smoothed, a *marching cubes* algorithm was used to reconstruct the outer surfaces. Then another meshing algorithm is used to fill the volume with tetrahedrons. The process of digital twin generation is illustrated in Fig. 4.

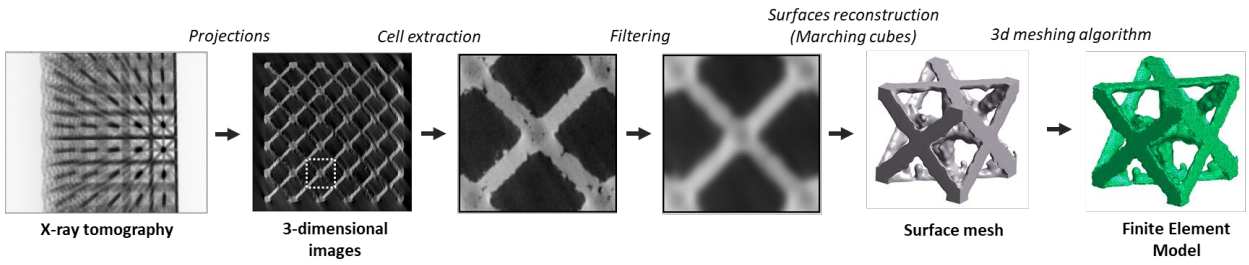

Fig. 4: Digital twin RVE creation process illustration.

In this work, six different cells were extracted from the same lattice sample. Using the previously described process, digital twins of our RVE are created, three of them are shown in Fig. 5. In addition, one *as-designed* RVE has been created for comparison purpose. The relative volumes of the RVEs are shown in Table 1. The RVEs FE models were created using DS Abaqus software using linear tetrahedral elements (C3D4). Each RVE is composed of approximately 1.6 * 10^5 elements. The material behavior for the RVE simulation was modeled using standard elastic-plastic law for aluminum with isotropic hardening.

Fig. 5: Three different as-manufactured RVEs from the same lattice sample.

Table 1: RVEs relative volumes.

RVE	Relative volume (%)
As-designed	16.58
As-manufactured #1	19.39
As-manufactured #2	19.46
As-manufactured #3	19.25
As-manufactured #4	19.56
As-manufactured #5	19.54
As-manufactured #6	18.12
As-manufactured mean	19.22

In this work the finite element method is used for the simulation the RVE problem. We note however that other methods exist, such as, Fast Fourier Transform, see [11]. These methods can be based directly on images without the necessity of building a mesh making them particularly efficient to model RVEs with large voids. Exploring this alternative is out of scope of this work but will be explored in future study.

Computational Homogenization. Localization of the macroscopic strain state on the RVE is performed by applying boundary conditions on its external surfaces Γ_D. The displacements field $\mathbf{q}_\Gamma$ of the nodes belonging to a face of the RVE's enveloping cube is constrained and driven to ensure a mean value of the RVE strain $\boldsymbol{\varepsilon}$. In the literature, three different types of boundary conditions (ensuring Hill-Mandel energy condition and allowing to impose an average deformation are used, namely, i) kinematic uniform, ii) uniform traction and iii) periodic boundary conditions.

The kinematic uniform boundary conditions are easy to implement and are used in this work. Here the displacements of the boundary nodes are driven by their position (Eq. 4). To that end, the displacements of the boundary nodes are driven by ε and by their position $\mathbf{X}_\Gamma$ as

$$\mathbf{q}_\Gamma = \boldsymbol{\varepsilon} \cdot \mathbf{X}_\Gamma \tag{4}$$

Materials Research Proceedings 41 (2024) 2182-2189 https://doi.org/10.21741/9781644903131-240

In order to describe the effective response of our RVEs and use it in MSDD approach we need to perform so-called meso-to-macro transition (Fig. 2). In our context, this simply boils down to the stress homogenization, that is, the macroscopic stress state $\boldsymbol{\sigma}$ becomes the volume average of the stress field $\boldsymbol{\sigma}_m$ [12] over the RVE volume (Eq. 5).

$$\boldsymbol{\sigma} = \langle \boldsymbol{\sigma}_m \rangle \quad \text{with} \quad \langle \bullet \rangle = \frac{1}{V_m} \int_{\Omega m} \bullet \, dv \tag{5}$$

For each strain state $\boldsymbol{\varepsilon}$ applied to the RVE, homogenized stresses are computed at 20 equally spaced increments. We note here that the input strain state $\boldsymbol{\varepsilon}$ is defined in 6-dimensional strain space. In order to limit the number of evaluation points exploring at the same time the strain space as much as possible, careful design of experiments is needed [13]. Thus, we exploit here the hypercube sampling and we choose to sample the strain space in three dimensions associated to the principal components of the strain tensor ε_I, ε_{II}, ε_{III}.

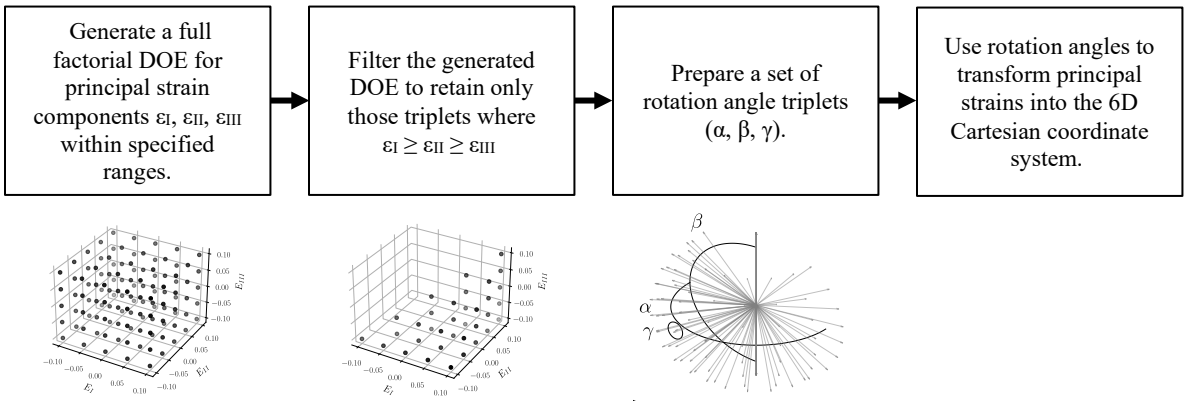

Fig. 6: Overview of used procedure to sample the 6D strain space.

The proposed sampling for this first attempt is made of 13 423 points of the strain space.

Results

As this work is still in progress, the performed simulations created a database that is currently composed of 5517 points related to 7 different RVEs: 6 related to *as-manufactured* and 1 to *as-designed* configuration. We recall that each of the material points is defined in 12-dimensional phase space Z with couples of strain and stress tensors ($\boldsymbol{\varepsilon}$, $\boldsymbol{\sigma}$). The evaluations and homogenization procedures are performed sequentially on a laptop Intel® Core™ i7-10510U CPU @ 1.80GHz with 32Gb memory. Projections on two of the 12 dimensions of Z enlighten the differences in mechanical response between the RVEs. Points resulting from unidimensional loading cases (only one component of the loading strain is non-zero) are presented in Fig. 7.

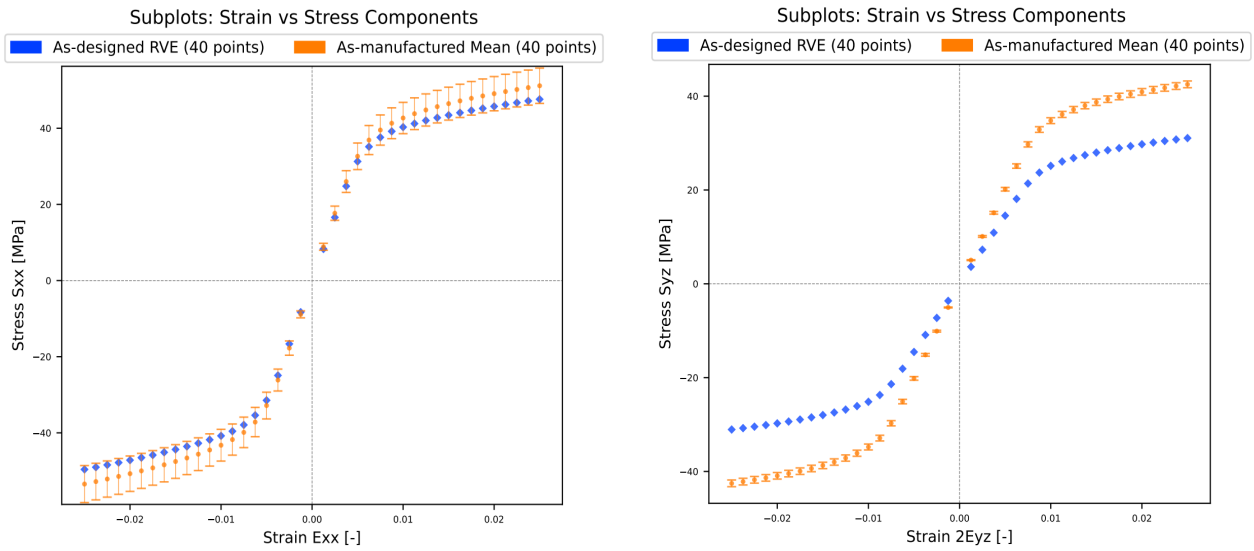

Fig. 7: Extract of data created by simulations on the 7 RVEs, showing the projected stress and strain values on the dimension of the phase space that corresponds to the loaded strain component. The results for the as-manufactured configuration are displayed with error bars showing the variability (the mean value and the standard deviation) of generated data from different RVE realizations.

As can be clearly seen from the presented examples, different geometries of the RVEs lead to variation in homogenized mechanical responses. The first noticeable difference is between the *as-designed* configuration (blue points in Fig. 7) and the average of the *as-manufactured* configurations. This systematic bias is associated both with the manufacturing process and the creation of the digital twins. Not surprisingly, different cells within the same lattice sample exhibit different defects, and therefore, do not demonstrate the same behavior. Consequently, for the *as-manufactured* RVEs, there is a random variability in the homogenized stress states. In Fig. 7, error bar type of plot is used for the graphical representation of the variability of the data. We note in passing that observed variability increases with the magnitude of the loading as shown in Fig. 7.

Discussion

The systematic bias in the stress response can be partly explained by the difference in relative volume. As presented in Table 1, the average relative volume of the *as-manufactured* configurations is increased by 15.9% compared to that of the *as-designed* configuration.

As a correlation between relative volume and mechanical response is expected, in forthcoming work, we will delve deeper into its influence and the origin of its deviation from the *as-designed* value. However, this difference can come either from a systematic bias related to the manufacturing process or from the digital twin creation procedure. The relative volume of the digital twins is influenced by the parameters of their creation process namely the cell extraction, filtering, surface reconstruction and meshing. One of the examples of significant parameter is the threshold of the marching cubes algorithm used to reconstruct the outer surfaces which impacts the relative density and the overall homogenized response. As mentioned previously, our perspective is to profit from the variability of responses from the *as-manufactured* configurations and to propose a database ‘filtering’ method. This method will consider the fact that variability is not identical in all loading directions and for different amplitudes of the loading.

References

[1] L. J. Gibson et M. F. Ashby, *Cellular Solids: Structure and Properties*. Cambridge University Press, 1997.

[2] B. Blakey-Milner et al., Metal additive manufacturing in aerospace: A review, Materials & Design, 209 (2021) 110008. https://doi.org/10.1016/j.matdes.2021.110008

[3] L. Riva, P. S. Ginestra, E. Ceretti, Mechanical characterization and properties of laser-based powder bed–fused lattice structures: a review, Int J Adv Manuf Technol, 113 (2021) 649-671, doi: 10.1007/s00170-021-06631-4

[4] L. Liu, P. Kamm, F. García-Moreno, J. Banhart, D. Pasini, Elastic and failure response of imperfect three-dimensional metallic lattices: the role of geometric defects induced by Selective Laser Melting, Journal of the Mechanics and Physics of Solids, 107 (2017) 160-184. https://doi.org/10.1016/j.jmps.2017.07.003

[5] F. Feyel, A multilevel finite element method (FE2) to describe the response of highly non-linear structures using generalized continua, Computer Methods in Applied Mechanics and Engineering, 192 (2003) 3233-3244. https://doi.org/10.1016/S0045-7825(03)00348-7

[6] B. A. Le, J. Yvonnet, et Q.-C. He, Computational homogenization of nonlinear elastic materials using neural networks, International Journal for Numerical Methods in Engineering, 104 (2015) 1061-1084,doi: 10.1002/nme.1586

[7] T. Kirchdoerfer et M. Ortiz, Data-driven computational mechanics, Computer Methods in Applied Mechanics and Engineering, 304 (2016) 81-101. https://doi.org/10.1016/j.cma.2016.02.001

[8] R. Xu et al., Data-driven multiscale finite element method: From concurrence to separation, Computer Methods in Applied Mechanics and Engineering, 363 (2020), 112893. https://doi.org/10.1016/j.cma.2020.112893

[9] A. Platzer, A. Leygue, L. Stainier, Stratégie adataptive de calcul multiéchelle piloté par les données, 15ème Colloque National en Calcul des Structures, mai 2022.

[10] R. Eggersmann, L. Stainier, M. Ortiz, et S. Reese, Model-free data-driven computational mechanics enhanced by tensor voting, Computer Methods in Applied Mechanics and Engineering, 373 (2021) 113499. https://doi.org/10.1016/j.cma.2020.113499

[11] H. Moulinec, P. Suquet, A numerical method for computing the overall response of nonlinear composites with complex microstructure, Computer Methods in Applied Mechanics and Engineering, 157 (1998) 69-94. https://doi.org/10.1016/S0045-7825(97)00218-1

[12] E. Sanchez-Palencia, Homogenization in mechanics: A survey of solved and open problems, Rend. Sem. Mat. Univers. Politecn. Torino, 1986.

[13] M. A. Bessa et al., A framework for data-driven analysis of materials under uncertainty: Countering the curse of dimensionality, Computer Methods in Applied Mechanics and Engineering, 320 (2017) 633-667. https://doi.org/10.1016/j.cma.2017.03.037